



Cause investigation of ground sliding during tunneling in sloping and stratified stratum

Yongxing Zhang^{1,2,3} · Maoqi Yuan¹ · Weihua Lu¹ · Jian Zhang²

Received: 28 February 2021 / Accepted: 29 October 2021 / Published online: 8 November 2021
© The Author(s), under exclusive licence to Springer Nature B.V. 2021

Abstract

This paper presents a case study of investigating the cause of ground sliding during tunneling in the mountain with sloping and stratified stratum, which is implemented by field investigation and numerical analysis. Especially, the strength reduction finite element method is adopted to numerically investigate the influence of surrounding rocks stability from heavy rainfall permeating into ground. Both the field and numerical investigations demonstrate that the ground sliding during tunneling in the sloping and stratified stratum is induced by heavy rainfall permeating into the mountain ground with sloping and stratified stratum, in which heavy rainfall is observed before ground sliding and the instability of mountain slope is reduced with the gradually decreased rainfall. Moreover, the numerical analysis demonstrates that the plastic zones of surrounding rocks in the case of tunneling work implemented later than heavy rainfall are less developed than those in the case of tunneling work implemented earlier than heavy rainfall, which also implies the heavy rainfall permeating into the mountain ground has significant influence on the ground sliding during tunneling in the sloping and stratified stratum.

Keywords Ground sliding · Sloping and stratified stratum · Tunneling · Heavy rainfall · Strength reduction finite element

1 Introduction

With the great increase in constructing infrastructure, tunnel has been extensively used in transportation engineering, since it has attractive advantages of saving precious ground as well as traversing obstacle of mountains and rivers, whereas landslides are easily appeared around the tunnel site (Wang et al. 2020a, b). In view of previous investigations, tunnels are often suffered from harsh geological condition of landslides areas (Minardo et al. 2018; Gattinoni et al. 2019; Chen et al. 2020a, b; Wang et al. 2020a, b) and seismic zones

✉ Yongxing Zhang
zhangyongxing81@aliyun.com

¹ School of Civil Engineering, Nanjing Forestry University, Nanjing 210037, China

² Key Laboratory of Ministry of Education for Geomechanics and Embankment Engineering, Hohai University, Nanjing 210024, China

³ School of Civil Engineering, Central South University, Changsha 410075, China

(Vanuvamalai et al. 2018; Okazaki et al. 2003), and topographical conditions of shallow depth and asymmetry pressure (Fu et al. 2014; Zhang et al. 2017a; Sun et al. 2018) as well as rainfall (Wei et al. 2019; Fan et al. 2020) and untreated cavities around surrounding rocks resulted from over excavation in tunneling (Zhang et al. 2015, 2017b; Zhao et al. 2019), which can easily induce landslides during tunneling (Chatziangelou and Christaras 2010; Zhou et al. 2020; Chen et al. 2020a, b). However, the cause of landslide during tunneling in field is not easy to be identified although various approaches are developed for investigation (Minardo et al. 2018; Chen et al. 2020a, b; Zhang et al. 2015), since it may be affected by not only single factor but also the coupled action of the aforementioned influencing factors. Therefore, further study related to landslide during tunneling in field is thus urgently required, which can provide the reference for determining the reasonable treatment with landslides occurred in tunnel site.

In this paper, a case study of investigating the cause of ground sliding during tunneling in the mountain with sloping and stratified stratum is presented by field investigation and numerical analysis, in which severe damages are observed in both ground surface and tunnel lining, and the strength reduction finite element method (SRFEM) is adopted to numerically simulate the instability of surrounding rocks influenced by heavy rainfall permeating into ground. Moreover, the simulation of two cases is conducted for clarifying the combined influence of tunneling and ground sliding from heavy rainfall permeating into ground, in which the tunneling work in case a is implemented earlier than heavy rainfall and similar with that in field construction, whereas that in case b is carried out after heavy rainfall.

2 Profile of the tunnel

2.1 Landform and geological condition around tunnel site

The tunnel is located in the landform of denuded middle and low mountain area built on the rock-soil boundary layer of the mountain, which has 10,743 m length and 515 m maximum buried depth. Figure 1 demonstrates the geological constitution around the tunnel with 9 geological drilling holes implemented for supplementary survey, which is situated in the steep terrain of hard-soft heterogeneous ground with sloping and stratified stratum, including fully-weathered and strongly-weathered as well as

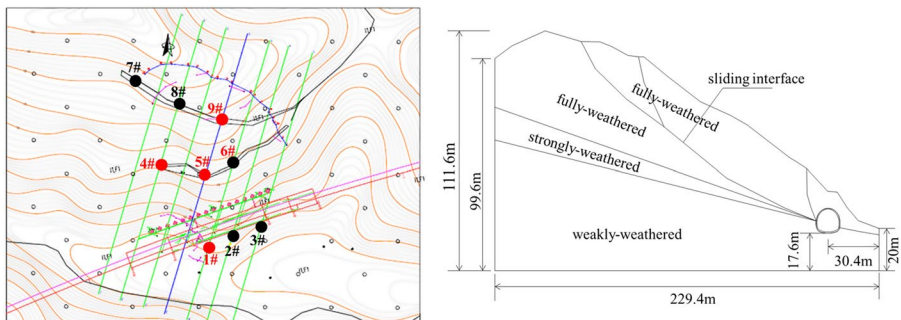


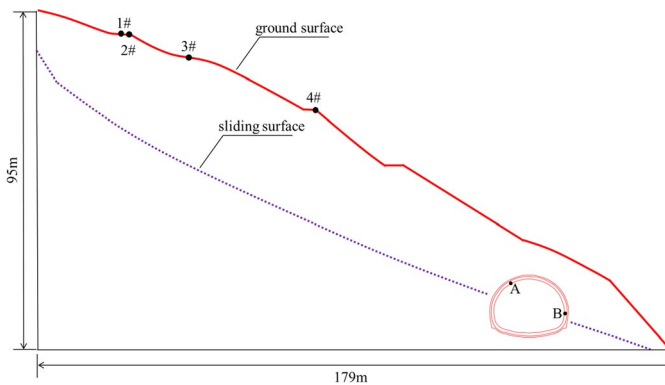
Fig. 1 Schematic geological condition around the tunnel

weakly-weathered mica-quartzose schist, respectively. Moreover, the tunnel is buried in a V-shape valley with shallow depth, and there is no visible water in the fissures of the rock strata. The tunnel entrance is along the mountain foot at the edge of the narrow and long valley, which is distributed in strips and seriously affected by atmospheric rainfall with severe rain erosion.

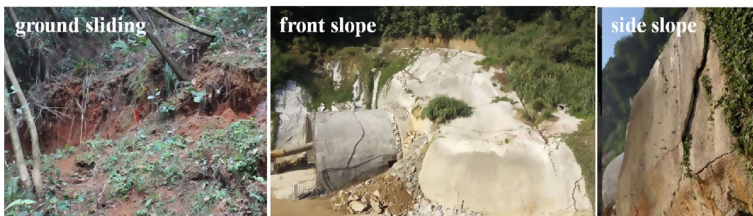
3 Field investigation of ground sliding during tunneling

3.1 Field observed ground sliding behavior

The field investigation is implemented to obtain the ground sliding during tunneling. Figure 2 demonstrates the field observed ground sliding with typical transfixion cracks in both ground surface and concrete lining of tunnel entrance, in which the transfixion cracks in ground surface are labeled as 1#, 2#, 3# and 4#, and those in concrete lining are labeled as A and B. As illustrated in Fig. 2b, several continuous cracks with 6 maximum width in concrete lining are linearly spread in longitudinal direction and distributed around the areas within the hance and sidewall, typical transfixion cracks are found in ground surface with the longitudinal lengths greater than 200 m as well as 0.25 m maximum crack width, and severe cracks are observed in the front and side slopes of the tunnel entrance. Especially, heavy rainfall is observed before ground sliding.



(a) Schematic drawing of field observed transfixion cracks



(b) Crack pattern and sliding in ground surface

Fig. 2 Field observed ground sliding with typical transfixion cracks in tunnel entrance

3.2 Field monitoring ground sliding

The sliding behavior of ground surface are monitored in field, in which 4 inclinometer pipes are adopted for measuring the horizontal displacement of ground, installed in the aforementioned geological drilling holes. Moreover, the positions of inclinometer pipes are labeled as 1#, 4#, 5# and 9# as marked in Fig. 1, in which 1# position is located in the tunnel's left sides within low-altitude area, 4#, 5# and 9# positions are respectively located in the tunnel's right sides within high-altitude area.

Figure 3 demonstrates the field measured relationship curves of horizontal displacement and depth at 1# and 4# drilling holes, in which the horizontal displacement of 4# drilling hole illustrates that the instability of mountain slope is reduced with the gradually decreased rainfall with 20-days measuring time. Moreover, the field measured average sliding rates of 1#, 4#, 5# and 9# drilling holes are 0.52 mm/day, 0.91 mm/day, 1.7 mm/day and 3.49 mm/day, respectively.

4 Numerical investigation of ground sliding during tunneling

4.1 Numerical model and material properties

Figure 4 demonstrates the numerical model as well as boundary condition, which is adopted for numerically investigating the cause of ground sliding during tunneling. In the numerical model, the longitudinal calculation range is 229.4 m, that of lateral side to the tunnel is 30.4 m, and the vertical calculation ranges of both lateral sides are 111.6 m and 20 m from top surface to lower boundary, respectively. Moreover, the assumptions in boundary conditions are marked in the model, in which the bottom boundary is fixed in both longitudinal and vertical directions, and both lateral boundaries are restricted in longitudinal direction, whereas upper boundary is free in both longitudinal and vertical directions.

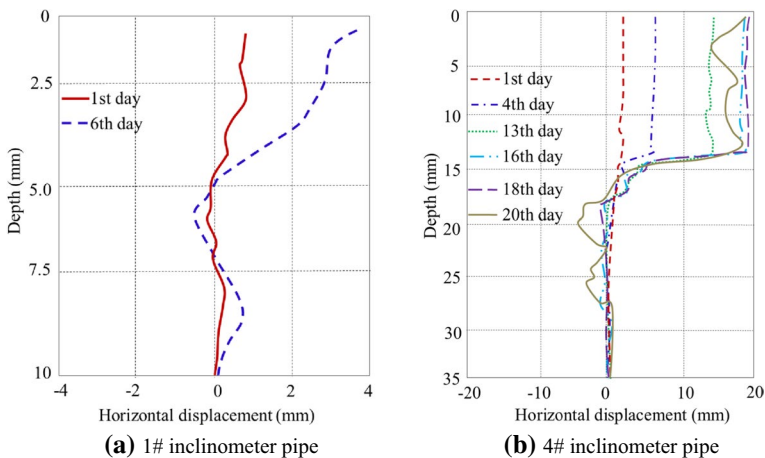
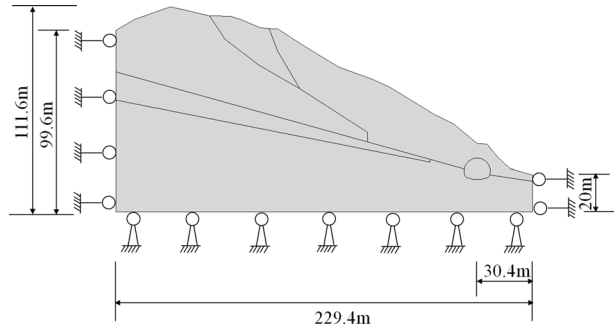


Fig. 3 Horizontal displacement versus depth of ground using inclinometer pipes

Fig. 4 Numerical model and boundary condition



The physical and mechanical properties of surrounding rocks and lining concrete are listed in Table 1, obtained from the aforementioned in situ supplementary survey with 9 geological drilling holes as well as laboratory test with 25 specimens, in which E and γ are elastic modulus and bulk density respectively, f_c' is concrete's compressive strength, μ is Poisson's ratio, c and φ are cohesive force and friction angle, respectively. Moreover, the surrounding rocks are considered as ideal elastic–plastic material met with Mohr–Coulomb yield criterion, which has been successfully adopted for reflecting the behavior of surrounding rocks during tunneling (Zhang et al. 2015).

4.2 Implementing numerical simulation using strength reduction finite element method

The ground sliding of the mountain during tunneling is numerically simulated using the strength reduction finite element method (SRFEM), in which the reduced strength of surrounding rocks are continuously adjusted by the following equations until the numerical sliding surface is similar with that in practice. Therefore, SRFEM can be adopted to reflect the influence of surrounding rocks stability from heavy rainfall permeating into ground, in which c_m and φ_m are the reduced cohesive force and friction angle, respectively; F_r is strength reduction coefficient.

$$\varphi_m = \arctan \left(\frac{\tan \varphi}{F_r} \right) \tag{1}$$

$$c_m = \frac{c}{F_r} \tag{2}$$

Table 1 Physical and mechanical properties of the materials

Material	Property parameters
Fully-weathered mica-quartzose schist	$E = 0.1 \text{ GPa}$, $\gamma = 22 \text{ kN/m}^3$, $\mu = 0.4$, $c = 0.05 \text{ MPa}$, $\varphi = 28.6^\circ$
Strongly-weathered mica-quartzose schist	$E = 3 \text{ GPa}$, $\gamma = 23 \text{ kN/m}^3$, $\mu = 0.3$, $c = 0.4 \text{ MPa}$, $\varphi = 30^\circ$
Weakly-weathered mica-quartzose schist	$E = 20 \text{ GPa}$, $\gamma = 25 \text{ kN/m}^3$, $\mu = 0.25$, $c = 1.0 \text{ MPa}$, $\varphi = 45^\circ$
Lining concrete	$E = 31.5 \text{ GPa}$, $\mu = 0.2$

In the numerical analysis, two cases are simulated for clarifying the combined influence of tunneling and ground sliding from heavy rainfall permeating into ground. Table 2 shows the conducted three steps in the simulated cases *a* and *b*, in which both cases have the same first step of balancing the ground stress with applying gravity and the calculated displacement is returned to zero for removing the adverse influence on sliding surface, and the tunneling work in case *a* is implemented earlier than heavy rainfall and similar with that in field construction, whereas that in case *b* is carried out after heavy rainfall.

4.3 Numerical result

4.3.1 Displacement and plastic zones of the mountain slope in case a

Figure 5 demonstrates the calculated relationship of the maximum displacement and strength reduction coefficient of the mountain slope. It can be clearly seen that the maximum displacements of the slope are varied little with the strength reduction coefficient smaller than 1.25, whereas it is rapidly increased with the increasing strength reduction coefficient thereafter, which means severe ground sliding occurs in the slope with the strength reduction coefficient larger than 1.25. This implies that the ground sliding during tunneling is probably influenced by heavy rainfall permeating into the ground of the mountain with sloping and stratified stratum.

Figure 6 shows the numerically obtained plastic zone distributions of surrounding rocks in case *a*, in which the cohesive force and friction angle are reduced from the original ones using the aforementioned strength reduction equations. It can be clearly seen that the numerically obtained main continuous sliding surface is similar with the ground sliding observed from field investigation, and the numerical calculated strength of the main continuous sliding surface has 0.02 MPa cohesive force and 34.9° friction angle, which confirms the effectiveness of the conducted numerical investigation. Moreover, the plastic zones of surrounding rocks are connected and developed along the main continuous sliding surface, which can form landslide in the mountain. This means that the field observed ground sliding during tunneling is induced by heavy rainfall permeating into the ground of the mountain with sloping and stratified stratum.

4.3.2 Plastic zones of the mountain slope in case b

Figure 7 demonstrates the numerically obtained plastic zone distributions of surrounding rocks in case *b*, in which the reduced strength of the main sliding surface in case *a* with 0.02 MPa cohesive force and 34.9° friction angle is adopted for implementing the numerical simulation. It is obvious that the plastic zones of surrounding rocks in this case still tend to be connected with a risk of forming landslide, whereas they are less developed than those in case *a* with tunneling work implemented earlier than heavy rainfall, even though the same strength of the main continuous sliding surface is adopted in numerical simulation. This also implies the heavy rainfall permeating into the mountain ground has significant influence on the ground sliding during tunneling in the sloping and stratified stratum.

Table 2 Conducted steps in the simulated cases

Case	Step	
	1	3
<i>a</i>	Balancing ground stress with applying gravity and clearing displacement	Excavating tunnel and adding concrete lining
<i>b</i>	Calculating slope stability with reduced strength of main sliding surface in case <i>a</i>	Calculating slope stability using SRFEM Excavating tunnel and adding concrete lining

Fig. 5 Maximum displacement of slope with strength reduction

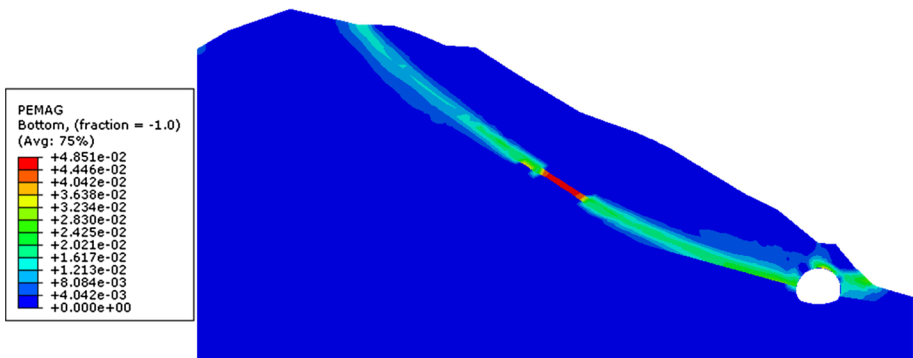
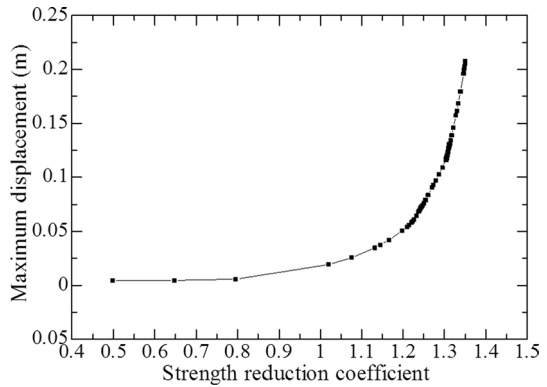


Fig. 6 Plastic zone distribution of surrounding rocks in case *a*

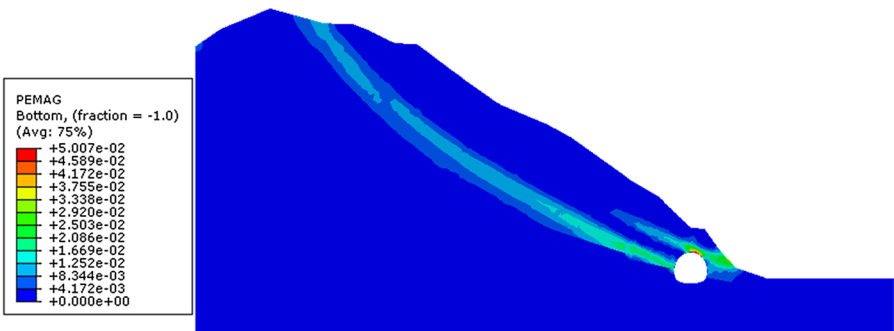


Fig. 7 Plastic zone distribution of surrounding rocks in case *b*

5 Conclusions

In this paper, a case study of investigating the cause of ground sliding during tunneling in the sloping and stratified stratum is implemented, and the following conclusions can be drawn:

- (1) Both the field and numerical investigations confirm that the ground sliding during tunneling in the sloping and stratified stratum is induced by heavy rainfall permeating into the mountain ground with sloping and stratified stratum, in which heavy rainfall is observed before ground sliding and the instability of mountain slope is reduced with the gradually decreased rainfall.
- (2) The numerical analysis demonstrates that the plastic zones of surrounding rocks in the case of tunneling work implemented later than heavy rainfall are less developed than those in the case of tunneling work implemented earlier than heavy rainfall, even though the same strength of the main continuous sliding surface is adopted in numerical simulation. This also implies the heavy rainfall permeating into the mountain ground has significant influence on the ground sliding during tunneling in the sloping and stratified stratum.
- (3) The strength reduction finite element method (SRFEM) can adopt to numerically simulate the instability of surrounding rocks influenced by heavy rainfall permeating into ground, the effectiveness of which is confirmed by field investigation and numerical analysis.

Funding The authors would like to acknowledge the support from Natural Science Foundation of Jiangsu Province (No. BK20211281), Open Fund of Key Laboratory of Ministry of Education for Geomechanics and Embankment Engineering (Hohai University), Six Talent Peak Projects.

Declarations

Conflict of interest The authors declare that there is no conflict of interest in the manuscript.

References

- Chatziangelou M, Christaras B (2010) Landslides and tunneling geological failures, during the construction of Thessaloniki-Kavala section of Egnatia highway in N Greece. *Int J Geol* 4:48–57
- Chen IH, Lin YS, Su MB (2020a) Computer vision-based sensors for the tilt monitoring of an underground structure in a landslide area. *Landslides* 17:1009–1017
- Chen ZQ, He C, Yang WB, Guo WQ, Li Z, Xu GW (2020) Impacts of geological conditions on instability causes and mechanical behavior of large-scale tunnels: a case study from the Sichuan-Tibet highway, China. *Bull Eng Geol Environ*. <https://doi.org/10.1007/s10064-020-01796-w>
- Fan SY, Song ZP, Zhang YW, Liu NF (2020) Case Study of the effect of rainfall infiltration on a tunnel underlying the roadbed slope with weak inter-layer. *KSCE J Civ Eng* 24:1607–1619
- Fu JY, Yang JS, Zhang XM, Klapperich H, Abbas SM (2014) Response of the ground and adjacent buildings due to tunnelling in completely weathered granitic soil. *Tunn Undergr Space Technol* 43:377–388
- Gattinoni P, Consonni M, Francani V, Leonelli G, Lorenzo C (2019) Tunnelling in landslide areas connected to deep seated gravitational deformations: an example in Central Alps (northern Italy). *Tunn Undergr Space Technol* 93:103100
- Minardo A, Catalano E, Coscetta A, Zeni G, Zhang L, Di Maio C, Vassallo R, Coviello R, Macchia G, Picarelli L, Zeni L (2018) Distributed fiber optic sensors for the monitoring of a tunnel crossing a landslide. *Remote Sens* 10:1291
- Okazaki J, Ogawa A, Tamura T (2003) A study on cracks of tunnel concrete lining in squeezing ground. *J Tunn Eng JSCE* 13:53–60

- Sun SQ, Li SC, Li LP, Shi SS, Wang J, Hu J, Hu C (2018) Slope stability analysis and protection measures in bridge and tunnel engineering: a practical case study from Southwestern China. *Bull Eng Geol Env* 78:3305–3321
- Vanuvamalai A, Jaya KP, Balachandran V (2018) Seismic performance of tunnel structures: a case study. *Nat Hazards* 93:453–468
- Wang XL, Lai JX, Qiu JL, Xu W, Wang LX, Luo YB (2020a) Geohazards, reflection and challenges in Mountain tunnel construction of China: a data collection from 2002 to 2018. *Geomat Nat Haz Risk* 11:766–785
- Wang XL, Lai JX, He SY, Garnes RS, Zhang YW (2020b) Karst geology and mitigation measures for hazards during metro system construction in Wuhan, China. *Nat Hazards* 103:2905–2927
- Wei ZL, Shang YQ, Sun HY, Xu HD, Wang DF (2019) The effectiveness of a drainage tunnel in increasing the rainfall threshold of a deep-seated landslide. *Landslides* 16:1731–1744
- Zhang YX, Shi YF, Zhao YD, Fu LR, Yang JS (2017a) Determining the cause of damages in a multi-arch tunnel structure through field investigation and numerical analysis. *J Perform Constr Facil* 31:04016104
- Zhang YX, Shi YF, Zhao YD, Yang JS (2017b) Damage in concrete lining of an operational tunnel. *J Perform Constr Facil* 31:06017002
- Zhang YX, Yang JS, Yang F (2015) Field investigation and numerical analysis of landslide induced by tunneling. *Eng Fail Anal* 47:25–33
- Zhao YD, Liu C, Zhang YX, Yang JS, Feng TG (2019) Damaging behavior investigation of an operational tunnel structure induced by cavities around surrounding rocks. *Eng Fail Anal* 99:203–209
- Zhou SH, Tian ZY, Di HG, Guo PJ, Fu LL (2020) Investigation of a loess-mudstone landslide and the induced structural damage in a high-speed railway tunnel. *Bull Eng Geol Env* 79:2201–2212

Publisher's Note Springer Nature remains neutral with regard to jurisdictional claims in published maps and institutional affiliations.